Dust generation in tokamaks: Overview of beryllium and tungsten dust characterisation in JET with the ITER-like wall

Dust Generation in Tokamaks: Overview of Beryllium and Tungsten Dust Characterisation in JET with the ITER-Like Wall

M. Rubel[a*], A. Widdowson[b], J. Grzonka[c,d], E. Fortuna-Zalesna[c], P. Petersson[a], Sunwoo Moon[a], N. Ashikawa[e], N. Asakura[f], Y. Hatano[g], K, Isobe[f], S. Masuzaki[e], H. Kurotaki[f], Y. Oya[h], M. Oyaidzu[f], M. Tokitani[e] and JET Contributors**

EUROfusion Consortium, JET, Culham Science Centre, OX14 3DB, Abingdon, UK
[a]Royal Institute of Technology (KTH), 10044 Stockholm, Sweden
[b]Culham Centre for Fusion Energy, Culham Science Centre, Abingdon, OX14 3DB, UK
[c]Warsaw University of Technology, 02-507 Warsaw, Poland
[d]Institute of Electronic Materials Technology, 01-919 Warsaw, Poland
[e]National Institute for Fusion Science, Toki, 509-5292, Japan
[f]National Institutes for Quantum, Radiological Science and Technology, Rokkasho, 039-3212, Japan
[g]Toyama University , Hydrogen Isotope Research Center, Gofuku, 3190, Toyama 930-8555, Japan
[h]Shizuoka University, 836 Ohya, Suruga-ku, Shizuoka 422-8529, Japan

**Corresponding author: marek.rubel@ee.kth.se*

Abstract

Operation of the JET tokamak with beryllium and tungsten ITER-like wall provides unique opportunity for detailed studies on dust generation: quantity, morphology, location, etc. The programme carried out in response to ITER needs for safety assessment comprises: (i) remotely controlled vacuum cleaning of the divertor; (ii) local sampling of loosely bound matter from plasma-facing components (PFC); (iii) collection of mobilized dust on various erosion-deposition probes located in the divertor and in the main chamber. Results of comprehensive analyses performed by a number of complementary techniques, e.g. a range of microscopy methods, electron and ion spectroscopy, liquid scintillography and thermal desorption, are summarized by following points:

(a) Total amount of dust collected by vacuum cleaning after three campaigns is about 1-1.4 g per campaign (19 - 26 h plasma operation), i.e. over 100 times smaller than in JET operated with carbon walls (i.e. in JET-C).

(b) Two major categories of Be dust are identified: flakes of co-deposits formed on PFC and droplets (2-10 μm in diameter). Small quantifies, below 1 g, of Be droplets and splashes are associated mainly with melting of beryllium limiters.

(c) Tungsten dust occurs mainly as partly molten flakes originating from the W-coated tiles.

Keywords: *JET tokamak, ITER-Like Wall, Dust, Beryllium, Tungsten*

***See author list of "Overview of the JET results in support to ITER", X. Litaudon et al., Nucl. Fusion, 57 (2017) 102001*

1. Introduction

Generation of dust particles in a reactor-class thermonuclear reactor is considered as a potential hazard which would create serious issues regarding safety and economy of operation. In the worst case of a massive water leak onto hot dust a pressure build-up and an explosion of the released hydrogen could occur. Air ingress may lead to ignition. Tritium-contaminated and neutron-activated dust is also a radiological hazard. Detailed knowledge of dust generation is important for licensing and future operation of ITER (International Thermonuclear Experimental Reactor). For that reason collection of loose matter and the determination of particle properties have been carried out since late nineties in most controlled fusion devices. A comprehensive list of references to studies performed until the end of year 2011 has been compiled by Braams [1]. It should be stressed, however, that most of those works originated from machines with plasma-facing components (PFC) made of carbon. The only exception was connected with dust studies at ASDEX Upgrade where the tokamak performance with the tungsten-coated wall has been tested [2,3]. Metal particles have been a target of studies also at other devices [4], but a new chapter in plasma-wall interactions has been open when the JET tokamak with tungsten and beryllium wall components came to the scene [5-7]. Operation of JET with the ITER-Like Wall (JET-ILW) composed of beryllium (Be) in the main chamber and tungsten (W) divertor provides unique opportunity to determine material migration and fuel retention under the ITER-relevant environment. This also includes detailed studies of dust generation: quantity, morphology, location in vessel, etc. The program carried out in response to the ITER needs for safety assessment comprises: (i) remotely controlled vacuum cleaning of the divertor; (ii) local sampling of loosely bound matter from PFC; (iii) collection of mobilized dust on various erosion-deposition probes located in the divertor and in the main chamber [8-11]. Until now, three ILW campaigns have been completed: ILW-1 (2011-2012); ILW-2 (2013-2014); ILW-3 (2015-2016). An important outcome of the surveys is related to a small amount of loose matter collected by vacuum cleaning: of the order of 1 g after each campaign, despite the fact that the total energy input per campaign was increasing: 150 GJ, 201 GJ and 245 GJ, respectively. The other findings are related to the identification of several categories of particles, both ITER-relevant and only JET-specific, and to the identification of several places from where metal droplets (mainly Be) were released.

Detailed studies require a broad range of techniques and a network of specialized laboratories with ability and expertise in: (i) analyzing of a broad spectrum of species, from hydrogen isotopes to tungsten; (ii) handling tritium and beryllium-contaminated materials. The aim of this paper is to provide a critical overview of the dust survey methods and results of comprehensive analyses, and to address modelling needs related to dust studies in JET-ILW.

2. Experimental

2.1 Dust survey and collection methods

After each ILW campaign a very detailed high-resolution photographic survey of all in-vessel components is carried out to determine the impact of plasma-wall interactions, especially off-normal events, on the state of PFC and possible damage to their structure. This facilitates the search for flaking (peeling-off) co-deposited layers and for splashes or droplets originated from melting of wall components. Images in Fig. 1(a) and (b) show examples of Be limiter melting and splashes of the ejected material. The photographic search is followed by vacuum cleaning of the divertor tiles. Dust is removed by a cyclone-type system from the divertor; surfaces of 22 out of 24 divertor modules are cleaned. Loose matter from the inner and outer legs is collected into separate pots. An image in Fig. 2(a) shows the equipment, while in Fig. 2(b) one finds the poloidal cross-section of the divertor with marked regions of cleaning. Further steps in dust sampling and preparation for analyses take place in the Beryllium Handling Facility (BeHF), where all materials retrieved from the torus are received. This comprises two remaining complete divertor modules equipped with erosion-deposition probes [12], selected limiter tiles, probes from the main chamber wall and also containers with the vacuumed dust. The latter is decanted into pots. Localised sampling of particles from the divertor and limiter components is carried out using carbon sticky pads, thus providing samples ready for analyses with electron and ion beam techniques. Sampling was done in over 120 locations on limiters and divertor tiles. In the following (in Section 3.2) only results for samples collected in the divertor will be reported.

Dust collection and sampling from the divertor carriers is also performed once the tiles have been removed. Monitors with silicon plates installed above the outer and inner divertor as well as various wall probes belong to a separate class of dust collectors. Images in Fig. 3 (a) and (b) show respectively a dust monitor and the silicon collector plate retrieved from JET. This type of monitors was developed and first tested in ASDEX Upgrade [3]. They enable studies of as-deposited particles, e.g. those mobilized, in a way undisturbed by the collection itself. The same applies to several other wall probes, such as test mirrors [12,13].

The methods described are complementary one to another, because each of them separately has clear advantages and serious drawbacks. A critical assessment of the dust survey and collection techniques is compiled in Table 1.

2. 2 Analysis procedure and methods

First steps in the analyses of vacuumed dust are related to the determination of: (a) radioactivity

level to infer the tritium content and activation; (b) mass of the collected matter and then the mass of the partion decanted to pots. The activity is measured at the Culham Science Centre also for all other samples (i.e. dust monitors, sticky pads) before their shipment for further studies [14].

Comprehensive analyses required a large set of techniques and it was carried out at several laboratories. Vacuumed dust was analyzed at the International Fusion Energy Research Centre (IFERC) at Rokkasho, Japan. Locally sampled species on carbon stickers and wall probes were examined at the Warsaw University of Technology, Poland, while the composition of deposits on wall probes was determined at the Ångström Laboratory of the Uppsala University, Sweden.

At IFERC surface morphology was determined by an optical microscope and a scanning electron microscope (SEM; Zeiss Ultra55) with energy dispersive X-ray spectroscopy (EDS). The chemical composition of dust particles surfaces was studied using X-ray photoelectron spectroscopy (XPS, PHI500 Versa Probe II, ULVAC-PHI Inc.). A magnesium source of 25 W was used with a spot diameter of 100 μm. Argon ion gun of 4 keV was used to etch the surfaces of dust particles to remove surface contaminants originated from the sample exposure to air. To enable SEM, EDS and XPS dust particles were fixed on a sticky copper tape. Nano-scale observations were conducted by the transmission electron microscope (TEM, JEOL JET-2100F). An atomic concentration on the cross-section was measured by electron probe micro analyzer (EPMA, JEOL JXA-8530F). Signals of EPMA are very sensitive to surface roughness, hence a dust particle was sectioned by a focused ion beam (FIB, Hitachi FB-2100) to prepare lamellae-type samples and to smooth their surface for further analysis.

Ion beam analyses (IBA) were done at the 5 MeV Tandem Accelerator Laboratory of Uppsala University. Light species deposited and co-implanted in dust monitors were measured by means of time-of-flight heavy ion elastic recoil detection analysis (ToF HIERDA) using a 12 MeV Si^{3+} beam. The probed depth and the depth resolution were 120 nm and 8-10 nm, respectively. In studies of test mirrors from JET-ILW a 36 MeV iodine ($^{127}I^{8+}$) beam was applied in ToF HIERDA, while a 2.5 MeV $^{3}He^{+}$ beam was applied for nuclear reaction analysis (NRA) to quantify deuterium. Several microscopy methods were used at the Warsaw University of Technology (Poland) to examine morphology of dust and surfaces of wall probes: scanning electron microscopy (SEM, Hitachi SU-8000 FE-SEM) combined with energy-dispersive X-ray spectroscopy using silicon drift detector (EDS, Thermo Scientific Ultra Dry) enabling beryllium detection. Focused ion beam system (FIB/SEM, Hitachi NB5000) was used to prepare lamellae-type cross-sections of co-deposits on mirrors from JET and the ion-irradiated region in the implanted mirrors. They were studied with a scanning transmission electron microscope (STEM, Hitachi HD2700) operated at the accelerating

voltage of 200 kV.

Retention and trapping characteristics of hydrogen isotopes in a small amount of dust particles (vacuumed cleaned matter) were evaluated by thermal desorption spectrometry (TDS) measurements. The release of molecules was measured with a quadrupole mass spectrometer at a heating rate of 0.5 K/s up to 1273 K. The analyzed particles could not be placed directly in the TDS vacuum chamber. Therefore, a few milligrams of matter was placed on a tantalum tray with an inner diameter of 8 mm and a depth of 1 mm, which was then inserted into the TDS system. This method was earlier used in analyses of dust particles from the JT-60U tokamak [15]. Quantitative tritium analysis was performed using liquid scintillography counting (LSC). In this analysis for ILW dust particles, limited amount of material, less than 1g, could be used. A polycarbonate membrane filter was used to catch (wipe-off) dust particles sticking to the inner wall of the glass pot due to static charge. Using a combination between the standard scintillation cocktail of Hionic Fluor (Soluene®-350) and the toluene base solution, polycarbonate membrane filters were dissolved before LSC analysis.

3. Results and discussion

3.1 Dust retrieved by vacuum cleaning

Microscopy (SEM) and EDS survey has identified a large variety of particles with respect to size and elemental composition (containing C, O, Ni+Fe+Cr, Al in addition to Mo, W,), but the main focus was on beryllium flakes from the co-deposited layers on the divertor tiles, such as reported in [7,10]. The examination of vacuumed grains was preceded by the selection process using radiography: imaging plate technique [16] to identify tritium-free and tritium-containing particles. It could be noticed that some particles, identified later as Be, did not contain tritium.

A survey performed with XPS has also confirmed the presence of a broad variety of elements and their chemical states. In the case of beryllium a spectrum the Be 1s core level exhibits two maxima thus clearly proving the coexistence of elemental beryllium (binding energy, E_B = 111.6 eV) and its oxide (BeO) with a chemical shift of 3 eV towards higher values of the binding energy. The data agree with those presented for laboratory samples [17] and the data for deposits on the JET-ILW divertor tiles [18,19].

Images and graphs in Fig. 4a-c are related to TEM studies of a FIB-sectioned 8 μm thick beryllium flake of a deposit. It most probably originates from the inner divertor: either from the high field gap closure plate (HFGC, i.e. Tile 0) or from the apron of Tile 1, because during the ILW-1

campaign deposits of that thickness had been formed only on those tiles, as reported in [20-22]. One perceives the fairly uniform bottom part of the deposit thus suggesting a quiescent columnar growth during the initial phase of the JET-ILW plasma operation with the L-mode. In that layer, the presence of only very few tungsten particles (encircled) has been identified with EDS. Their origin is related to the erosion of tiny flakes from the tungsten coatings on carbon fibre composite tiles (W-CFC). The number of tiny particles (5-15 nm), seen as white inclusions, has been increasing during the campaign due the increased power of auxiliary heating by neutral beam injection (NBI). From the electron diffraction pattern (Fig. 4b) recorded for the bottom part of the deposit one determines the lattice constant of a = 2.4 Å, i.e. close to the reference data for metallic beryllium, a = 2.264 Å; the reference pattern is in Fig. 4(c).

A thermal desorption spectrum for deuterium in dust particles (4.4 mg sample) is shown in Fig.5. The total deuterium retention determined mainly from the mass 4 signal of D_2 is 5.2 x 10^{18} D atoms, while the average retention in dust particles from the inner divertor has been estimated at the level of 1.2 x 10^{21} atoms/g. In the 2011-2012 JET campaign approximately 1.7 x10^{26} D atoms were puffed and 3.7 x 10^{23} D atoms were retained (0.2 %) mainly in the Be deposition layers at the inner divertor [23]. Total retained D in dust particles is estimated to be 8.2 x10^{20} D atoms in the inner divertor (only around 0.4 % of the retention in the divertor tile surface) which may indicate that the retention in metal dust is relatively small. It should be noted that D desorption is increased at the high temperature (> 800 K) and peaked at 1050 K, which does not appear in the standard beryllium deuteride powder [24]. It indicates the necessity to investigate further of relationship between hydrogen isotope retention, and surface morphologies and oxidations on JET-ILW dust particles. Tritium activity determined with liquid scintillography in a sample of 2.3 mg has been on the level of 0.1 GBq/g, equivalent to 2.8x10^{-7} g(T)/g or 56x10^{15} T atoms/g. , It should be stressed that some particles placed in the cocktails remained after the LSC analysis thus indicating the presence of insoluble fraction in the dust.

3.2 Local sampling: Dust collected on adhesive carbon pads

The morphology of particles found in the divertor has been diversified, as reported in [11]: beryllium-rich flakes of co-deposits and flakes detached from the Be-coated tiles of the inner wall cladding; Be droplets, tungsten flakes and nickel or Inconel droplets. The following section will be focused on fine structural details of Be and W particles extracted from surfaces of the tiles and from divertor carriers.

The appearance and internal structure of tungsten dust is shown in Fig. 6 (a-f) for a flake of the W coating on CFC tiles. One perceives a recrystallized melt zone (Fig. 6a) and the structure of grains

inside the material (Fig. 6b-d). Bright and dark spots (dependent on the STEM operating mode) visible in the images indicate holes in the structure. Defects such as dislocations and dislocation loops are shown in high-resolution images (Fig. 6e,f). It should be stressed that tungsten dust originated mostly (or even only) from the erosion W coatings. There has been no evidence of droplets or splashes.

Images in Fig. 7 (a-g) shows general appearance and very fine features of a beryllium-based co-deposit found after the second ILW campaign on the divertor carriers thus indicating that it was originally detached from the deposition zone on the tiles. Its composition was determined by EDS: Be as the main component with some carbon, oxygen, nitrogen and small quantities of Ni, Fe and W. The collection of images is a result of examination performed using SEM (Fig. 7 a-c) and STEM operated in different modes (Fig. 7 d-g). The sample for STEM was prepared using FIB technique. There are two main features: (i) relatively large size (over 350 μm) of a flake thicker than 30 μm and (ii) very porous structure visible both in the surface layer and inside the material. From STEM images one may conclude that the internal porosity exceeds 50%. It may be even greater taking into account that there are hollow elements in the structure. They resemble nano-tubes, as shown in Fig. 7(g). Based on that and assuming 65% porosity one may tentatively estimate the density of such Be-rich matter at the level of about 0.6 g cm^{-3}. High porosity of co-deposits on the divertor tiles can also be inferred from FIB-TEM analysis reported in [25,26]. These findings of low-density materials may partly explain very low weight of the matter collected by vacuum cleaning.

The results presented respectively in Figures 4(a) and 7(e-g) clearly demonstrate a significant structural differences and diversity of deposits: low porosity related to quiescent growth in the L-mode operation at the beginning of ILW-1 and highly porous structure following high-power operation in ILW-2. It is not possible to determine (even to speculate) the place where exactly the porous deposit was formed in the tokamak.

3.3. Particles deposited on dust monitors and test mirrors

Two main types of stuff have been found on the monitors: co-deposit resulting from material migration in JET and a variety of dust particles. Plots in Fig. 8 (a) are depth profiles determined by HIERDA for species deposited on the silicon substrate located above the inner divertor. The main constituents of the deposit are: Be, C, N, Ni+Fe and fuel atoms. There are only traces of tungsten. For clarity of the graph not all species are plotted. The layer thickness is around 300-350 nm. Its appearance is shown in Fig. 8(b), which clearly demonstrates the presence of fine dust particles (areal density approx. 400-500 cm^{-2}) and flaking of that layer. The latter is caused by an internal stress in the co-deposit most probably related to thermo-mechanical incompatibility between the

substrate and the layer. This statement is based on the fact that there are numerous blisters, 4 – 60 μm in diameter, which break. This observation proves that there is no critical thickness at which co-deposits start peeling-off. It shows that even very thin layers can detach thus generating brittle flakes of dust which may disintegrate further. It also should be mentioned that remnants of such flakes have not been detected on the plate by high-resolution SEM. Similar situation had been noticed on surfaces of test mirrors from JET where stratified carbon-rich [27,28] or beryllium-rich [11] co-deposits were peeling-off. In the latter case only few fragments of the broken layers remained on the mirror surface. This indicates that this type of dust does not adhere to surfaces on the contrary to other particles found on dust monitors and other wall probes, reported in [12,14]. In the following only a brief account on such objects will be given.

Images in Fig. 9 show examples of droplets, splashes and also irregular pieces of medium-Z and high-Z metals on the dust monitors and test mirrors: Ni, Cu, W. Nickel, the main component of Inconel alloy, originates most probably from the grills of antennas for auxiliary plasma heating and also possibly from damaged tie rods in Tile 7 from the outer divertor. Micrographs (Fig. 9 a and b) indicate that the material was molten before reaching the surface of the dust collector. The presence of small chunks of copper (Fig. 9 c) can be related to the erosion from grids of the neutral beam injection system. Spherical tungsten particle is not a droplet, but an agglomerate of tiny flakes (200 nm - 1 μm) detached from the W-coated tiles. It has a form of a ball with empty interior, as it was proven using FIB [10]. One can perceive seam-like features, indicated by arrows, between respective elements of the structure. This type of dust is quite common in JET, while the study has not provided any evidence of solid W droplets ejected as a result of material melting. The presence of spherical tungsten agglomerates has been identified on the monitors and also on mirrors located in the divertor. A possible pathway of formation has been discussed in [14]. Such objects have been found in JET and also in ASDEX Upgrade [3], i.e. in machines with W-coated tiles. In this sense, they may be considered not ITER-relevant, as no coated tiles will be placed in that machine. However, in ITER one may expect W-rich co-deposits. The question is whether flaking of such layers would lead to their coagulation in the plasma edge and, eventually, to the formation of ball-type dust or even small droplets. As a remark on W droplets in JET-ILW one should mention that the only exception is related to their formation on protruding components as seen during the dedicated melt experiment on intentionally misaligned lamellae in bulk tungsten tile at the divertor base, i.e. Tile 5 [29].

Beryllium on dust monitors and other wall probes occurs in the form of circular flat splashes (Fig. 10 a and b) and droplets regular of regular spherical or oval shape (Fig. 10 c and d). Their formation most probably occurred in the very last stage of operation in ILW-2, when experiments on

run-away electron generation were carried out. This resulted in melting of the upper dump plates and, as a consequence, ejection of molten matter. Surfaces of droplets are not smooth, but they reveal additional features, like cavities (100-200 nm in diameter, Fig. 10 c) or bubbles/blisters, 100-250 nm in diameter, as shown in Fig. 10 (d). In the latter case one also perceives regular and directional forms like fish scale (or wavy-like) suggesting the flow of material during the cooling phase. The fact is certainly not surprising, but this the first so clear documentation of such structures on Be dust. In Fig. 10 (e) there is FIB-produced cross-section which reveals the structure of thin-wall (45-50 nm) bubbles in a Be-rich deposit from the inner divertor, while the image in Fig. 10 (f) shows a large number of bubbles on the surface of a Be splashed on the test mirror from the main chamber wall. The results strongly suggest boiling state and partial evaporation of beryllium released from the limiters.

4. Concluding remarks

The procedures for dust collection and sampling together with a broad range of analysis methods described above constitute the most comprehensive approach to dust studies ever applied in a tokamak, especially in a machine with PFC containing hazardous substances, like those in JET. The overall objective was to provide the information on major processes leading to dust generation and reveal their qualitative and quantitative aspects. This does not lead to direct prediction or scaling of the total dust generation in a next-step machine, especially in the case of powerful off-normal events, The study shows that regular quiescent operation does not result in a massive production of debris. The common feature of all metal droplets and splashes is their small size, in a micrometer range, and good adherence to substrates. As a result, there is low weight of loose matter collected after each ILW campaign by vacuum cleaning of the divertor. It should also be stressed that no dust accumulation has been found in the grooves of castellated beryllium limiters, where only thin deposits were formed [30].

The work demonstrates high value of wall probes in the identification of particles. In some cases, like Be droplets and splashes, the analysis of probes helps tracking back the history and place of particles' origin. This probably should be taken into account when planning the construction and location of removable probes in ITER [30] Results from dust monitors and wall probes form the best-available data set for modelling. In particular, following topics can be considered: (i) generation and transport of droplets resulting from run-away electron events; (ii) formation transport of tungsten ball-like structures and, in general, (iii) dust transport to shadowed regions in the divertor. In addition, data from analysis of the vacuumed dust (i.e. small amount and diversity of forms) together with ex-situ analyses of PFC [9,25,32,33] create basis for comparison with dust observations in plasma and

for modelling the behavior of the ablated impurities in plasma.

Acknowledgement

This work has been carried out within the framework of the EUROfusion Consortium and has received funding from the European Union's Horizon 2020 research and innovation programme under grant agreement number 633053. The views and opinions expressed herein do not necessarily reflect those of the European Commission. Authors wish to thank the QST staff in Rokkasho and in Tokai for their support of this work. This work has been supported by the ITER Broader Approach Activity. The work has been partly supported by the Swedish Research Council (VR), Grant 2015-04844 and also by Ministry of Science and Higher Education of Poland from financial appropriations for science of the year 2017, granted for the implementation of the international co-financed project.

References

1. B. Braams, *Characterisation of Size, Composition and Origins of Dust in Fusion Devices*, IAEA, 2012, *http://www-nds.iaea.org/reports-new/indc-reports.*
2. E. Fortuna-Zalesna et al., *Characterization of dust collected after plasma operation of all-tungsten ASDEX Upgrade*, Phys. Scr. T159 (2014) 014066.
3. M. Balden et al., *Dust investigations in ASDEX Upgrade*, Nucl. Fusion 54 (2014) 073010.
4. E. Fortuna-Zalesna et al., *Dust survey following the final shutdown of TEXTOR: metal particles and fuel retention*, Phys. Scr. T167 (2016) 014059.
5. G.F. Matthews et al., *JET ITER-like wall – overview and experimental programme*, Phys. Scr. T145 (2011) 014001.
6. S. Brezinsek et al., *Beryllium migration in ITER-Like Wall plasmas*, Nucl. Fusion 55 (2015) 063021.
7. X- Litaudon and JET Contributors, *Overview of the JET results in support to ITER*, Nucl. Fusion 57 (2017) 102001.
8. A. Widdowson et al., *Material migration patterns and overview of first surface analysis of the JET ITER-like wall*, Phys. Scr. T159 (2014) 014010.
9. A. Baron–Wiechec et al., *First dust study in JET with the ITER-like wall: sampling, analysis and classification*, Nucl. Fusion 55 (2015) 113033.
10. E. Fortuna-Zalesna et al. *Studies of dust from JET with the ITER-Like Wall: Composition and internal structure*, Nucl. Mater. Energ 12 (2017) 582.
11. E. Fortuna-Zalesna et al., *Fine metal dust particles on the wall probes from JET with the ITER-Like Wall*, Phys. Scr. T170 (2017) 014038.
12. M. Rubel et al., *Overview of erosion–deposition diagnostic tools for the ITER-Like Wall in the JET tokamak*, J. Nucl. Mater. 438 (2013) S1204.
13. M. Rubel et al., *Metallic mirrors for plasma diagnosis in current and future reactors: tests for ITER and DEMO*, Phys. Scr., T170 (2017) 0140…
14. A. Widdowson et al., *Experience of handling beryllium, tritium and activated components from JET ITER-like wall*, Phys. Scr. T167 (2013) 014057.
15. N. Ashikawa et al., *Charactaristics of tungsten and carbon dusts in JT-60U and evaluation of hydrogen isotope retention*, J. Nucl. Mater. 438 (2013) S659.
16. Y. Hatano et al., *Tritium distribution on tungsten and carbon tiles used in the JET divertor*, Phys. Scr. T167 (2016) 014009.
17. C.F. Mallison and J.E. Castle, *Beryllium and Beryllium Oxide by XPS*, Surf. Sci. Spectra 20 (2013) 86. http://avs.scitation.org/doi/10.1116/11.20130701
18. S. Masuzaki et al., *Analyses of Structure, Composition and Retention of Hydrogen Isotopes in Divertor Tiles of JET with the ITER-Like Wall*, Phys. Scr. T170 (2017) 014031.
19. Y. Oya et al., *Correlation of surface chemical states with hydrogen isotope retention in divertor tiles of JET with ITER-Like Wall*, Fusion Eng. Des., submitted.
20. P. Petersson et al., *Co-deposited layers in the divertor region of JET-ILW*, J. Nucl. Mater. 463 (2015) 814.

21. J. Likonen et al., *First results and surface analysis strategy for plasma-facing components after JET operation with the ITER-like wall,* Phys. Scr. T159 (2014) 014016
22. M. Mayer et al., *Erosion and deposition in the JET divertor during the first ILW campaign,* Phys. Scr. T167 (2016) 014051.
23. K. Heinola et al., *Long-term fuel retention in JET ITER-like wall,* Phys. Scr. T167 (2016) 014075.
24. R. Doerner et al., *The role of beryllium deuteride in plasma-beryllium interactions,* J. Nucl. Mater. 390-391 (2009) 681.
25. M. Tokitani, et al., *Micro-/nano-characterization of the surface structures on the divertor tiles from JET ITER-like wall,* Fusion Eng. Des. 116 (2017) 1.
26. M. Tokitani, et al., *Plasma-wall interaction on the divertor tiles of JET ITER-like wall from the viewpoint of micro/nanoscopic observations,* Fusion Eng. Des., submitted. (these proceedings).
27. M. Rubel et al., *An overview of a comprehensive First Mirror Test in JET for ITER,* J. Nucl. Mater. 390-391 (2009) 1066.
28. M. Rubel et al., *Overview of the second stage in the comprehensive mirror test in JET,* Phys. Scr. T145 (2011) 014070.
29. J. Coenen et al., *Transient induced tungsten melting at the Joint European Torus (JET),* Phys. Scr. T170 (2017) 014 013.
30. M. Rubel et al., *Fuel inventory and deposition in castellated structures in JET-ILW,* Nucl. Fusion 57 (2017) 066027.
31. Ph. Mertens et al., *Removable samples for ITER – a feasibility and conceptual study,* Phys. Scr. T159 (2014) 014004.
32. P. Petersson et al., *Co-deposited layers in the divertor region of JET ILW,* J. Nucl. Mater. 463 (2015) 814.
33. A. Widdowson et al., *Overview of fuel inventory in JET with ITER-like wall,* Nucl. Fusion 57 (2017) 086045.

Table 1. Assessment of methods used at JET for dust survey and collection.

Method	**Advantages**	**Drawbacks and implications**
Vacuum cleaning	• Total amount of loosely bound matter in the divertor. • Sampling for TDS (the only option).	• Not possible to correlate dust morphology with the place of particles location. • Possible disintegration of particles. • Difficulty in the isolation of an object for detailed studies.
Sampling by sticky carbon pads	• Local sampling; area of 5 cm^2. • Good adhesion of collected matter to the sampler.	• Force is applied in collection process. Particles may get disintegrated and more than loose matter is or may be collected, i.e. co-deposits. • The examined surface represents bottom part of particles or co-deposits. • Difficulty in the determination of particles' shape and size, as they are embedded in glue. • Uncertainty with respect to completeness of collection as some, especially bigger, particles may be lost in the transportation of tiles from the torus to BeHF
Sampling by filter paper (wiping)	• Sampled area of 20-50 cm^2 • Effective collection of very small particles sticking well to surfaces, also by van der Vaals forces.	The same as for carbon stickers. The main difference is that the collected particles are embedded in cellulose, not in glue.
Dust monitors: Silicon plates	• Localised collection of dust undisturbed and not modified upon the collection: size and shape determination. • Possible conclusions on dust mobilization and adhesion.	Uncertainty with respect to completeness of collection as some, especially bigger, particles may be lost in the transportation of monitors from the torus to BeHF and then to analytical equipment.
Other wall probes	• Localized collection in many places in the main chamber and divertor on mirrors from the First Mirror Test [13], spatial blocks, cover plates of quartz microbalance devices. • Advantages as in the case of dust monitors.	The same as for dust monitors.
Photographic survey	• Most comprehensive record of wall modification by plasma-wall interactions. • Identification and mapping of droplets/splashes.	• No analyses, no information the on composition. Only "educated" guess is possible. • Risk for misjudgment (over- or underestimation) of the particle type and amount.

Figure captions

Figure 1

Melt zones on beryllium plasma-facing components: (a) upper dup plates; (b) inner wall guard limiters.

Figure 2

(a) Cyclone-type vacuum cleaner used in JET and (b) a poloidal cross-section of the divertor with areas of cleaning in the inner and outer leg.

Figure 3

Dust monitors in JET-ILW: (a) a schematic drawing of the monitor for the outer divertor; (b) silicon plate, i.e. the actual dust collector after exposure in JET.

Figure 4

TEM examination of the Be flaking co-deposit retrieved from JET by vacuum cleaning. (a) details of the deposit structure and content of tungsten particles at different depth corresponding to consecutive phases of operation during ILW-1. (b) electron diffraction recorded at the lower region of the deposits; (c) diffractogram for reference beryllium.

Figure 5.

Thermal desorption spectrum of deuterium from a sample of dust retrieved by vacuum cleaning from the inner divertor.

Figure 6

Surface topography and internal structure of tungsten dust sampled by sticky pads from the outer divertor tile recorded by SEM and STEM: (a) SEM image of surface features; (b) - (d) STEM images revealing details of the crystalline structure and porosity, (e) and (f) high resolution STEM revealing defects: dislocations and dislocation loops.

Figure 7

Thick beryllium deposits retrieved from the divertor carriers: (a) – (c) surface topography recorded by SEM and (d)-(g) internal structure recorded by STEM from the FIB-produced lamellae. Images (e) and (g) recorded in secondary electron mode, while (d) is high angle annular dark field image and

(f) is a bright field image.

Figure 8.

Analysis of silicon plate of the dust monitor from the inner divertor: (a) HIERDA-based depth profiles of co-deposit constituents on the plate; (b) overview SEM image of the Si plate with deposited dust particles and the peeling-off layer the co-deposit.

Figure 9.

SEM images of medium-Z and high-Z metal particles on the dust monitor: (a) and (b) nickel (Inconel) droplet and splash; (c) copper particle and (d) tungsten spherical particle formed the agglomeration of flakes from W-coated CFC tiles.

Figure 10.

SEM images of beryllium droplets and splashes: (a) splash on the dust monitor from the inner divertor (a); splash on the test mirror from the main chamber (b); droplets with surface features indicating the presence of cavities (c) and (d) small bubbles; (e) FIB-produced cross-section revealing the structure of thin-wall bubbles in a Be-rich deposit from the inner divertor; (f) bubble-like structure on the Be splash on the test mirror.

Figure 1

Melt zones on beryllium plasma-facing components: (a) upper dup plates; (b) inner wall guard limiters.

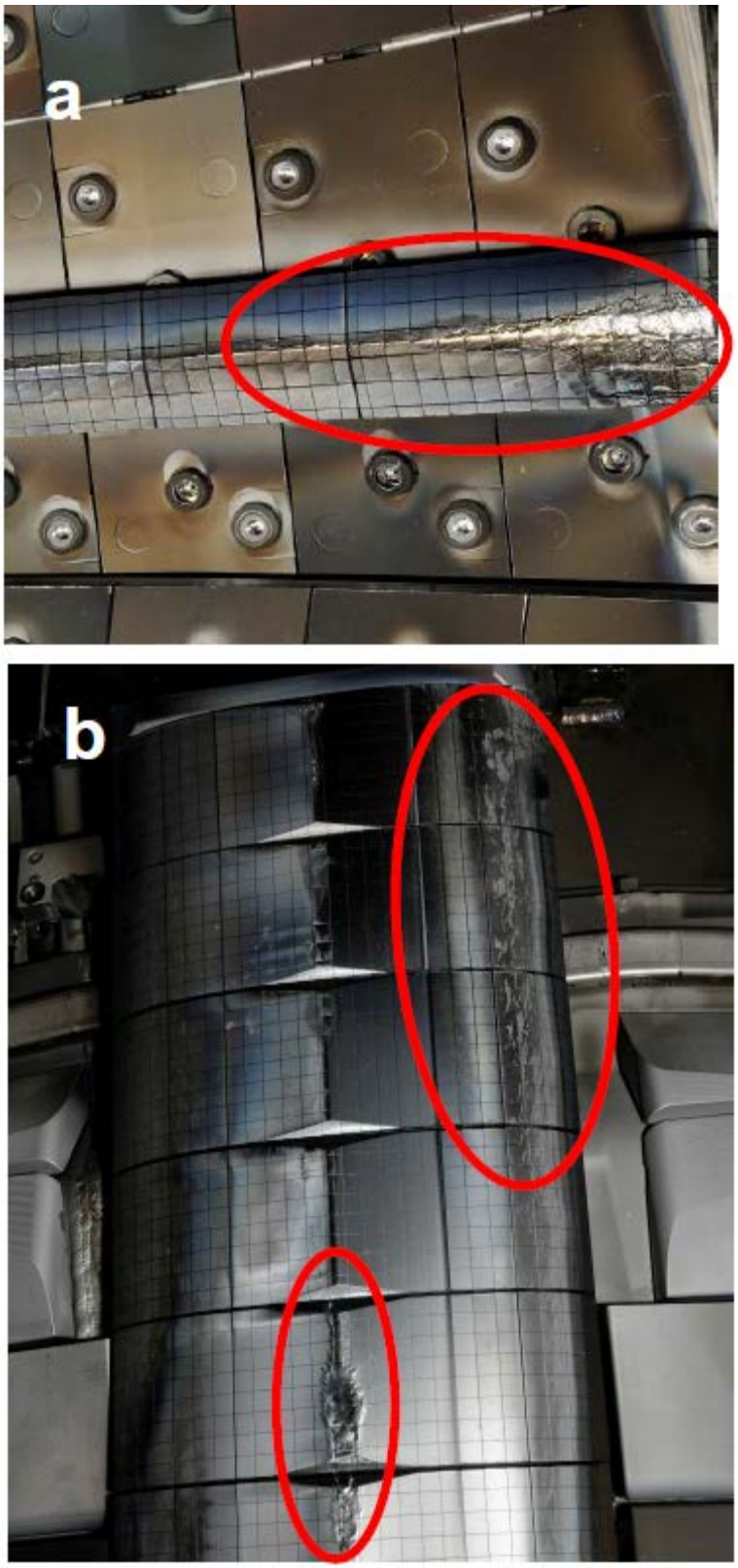

Figure 2

(a) Cyclone-type vacuum cleaner used in JET and (b) a poloidal cross-section of the divertor with areas of cleaning in the inner and outer leg.

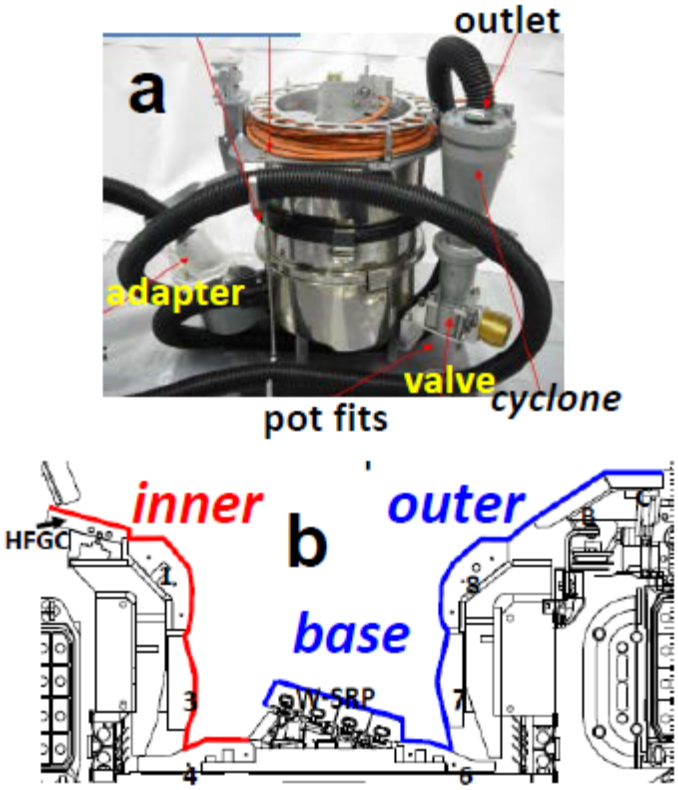

Figure 3

Dust monitors in JET-ILW: (a) a schematic drawing of the monitor for the outer divertor; (b) silicon plate, i.e. the actual dust collector after exposure in JET.

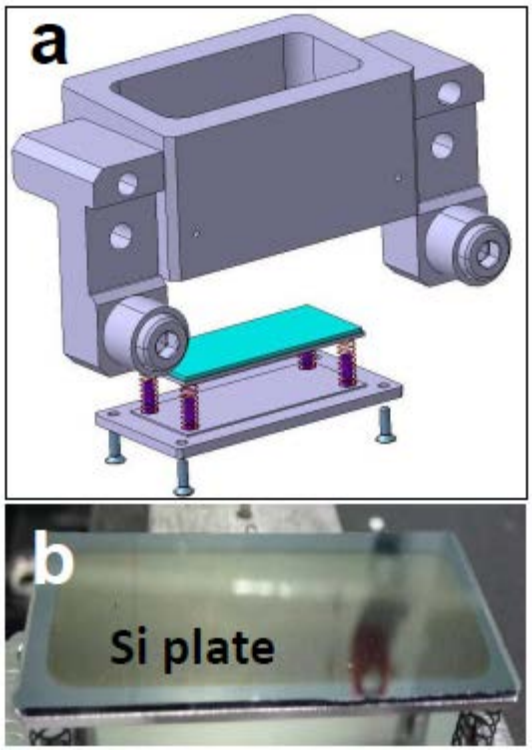

Figure 4

TEM examination of the Be flaking co-deposit retrieved from JET by vacuum cleaning. (a) details of the deposit structure and content of tungsten particles at different depth corresponding to consecutive phases of operation during ILW-1. (b) electron diffraction recorded at the lower region of the deposits; (c) diffractogram for reference beryllium.

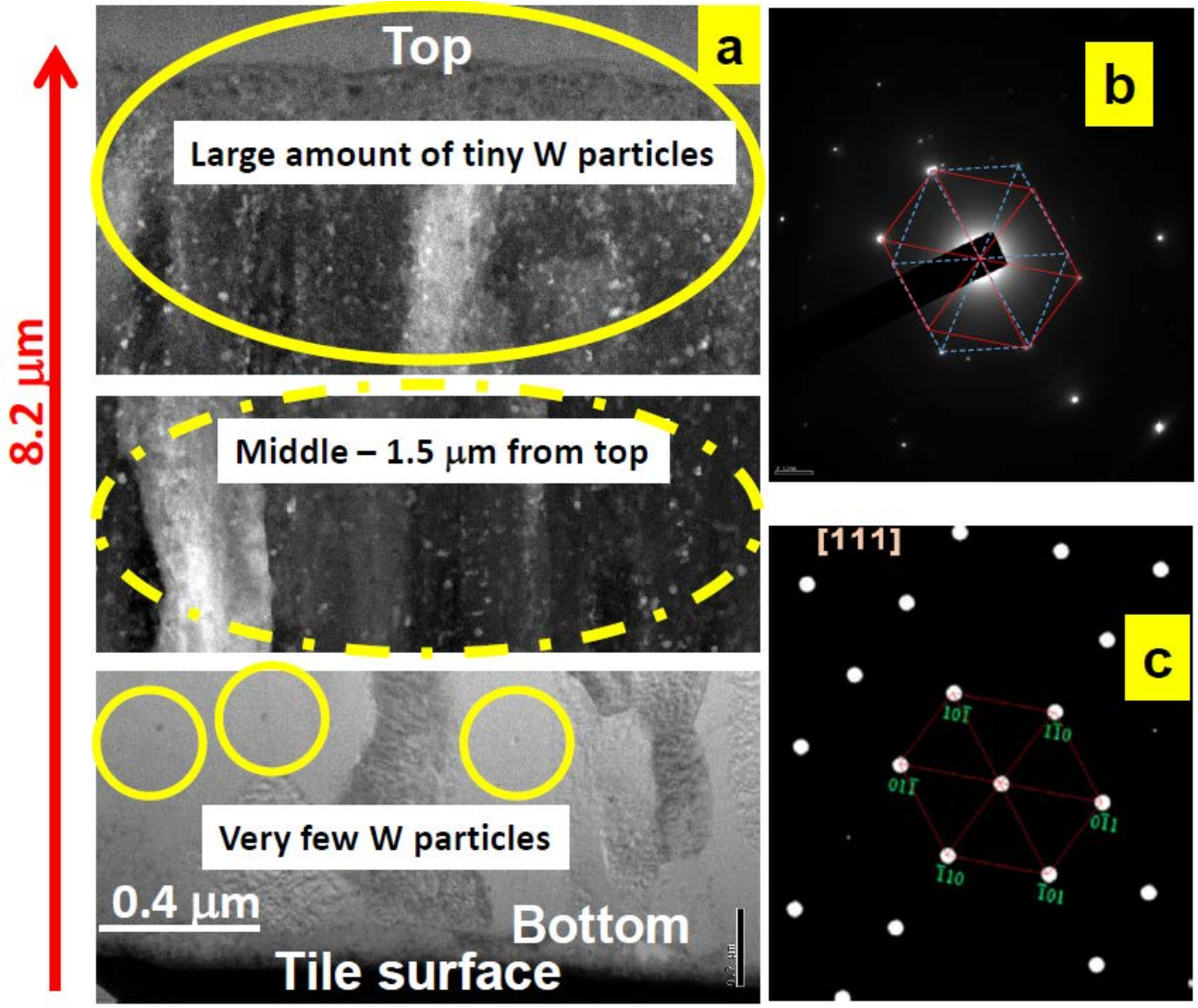

Figure 5.

Thermal desorption spectrum of deuterium from a sample of dust retrieved by vacuum cleaning from the inner divertor.

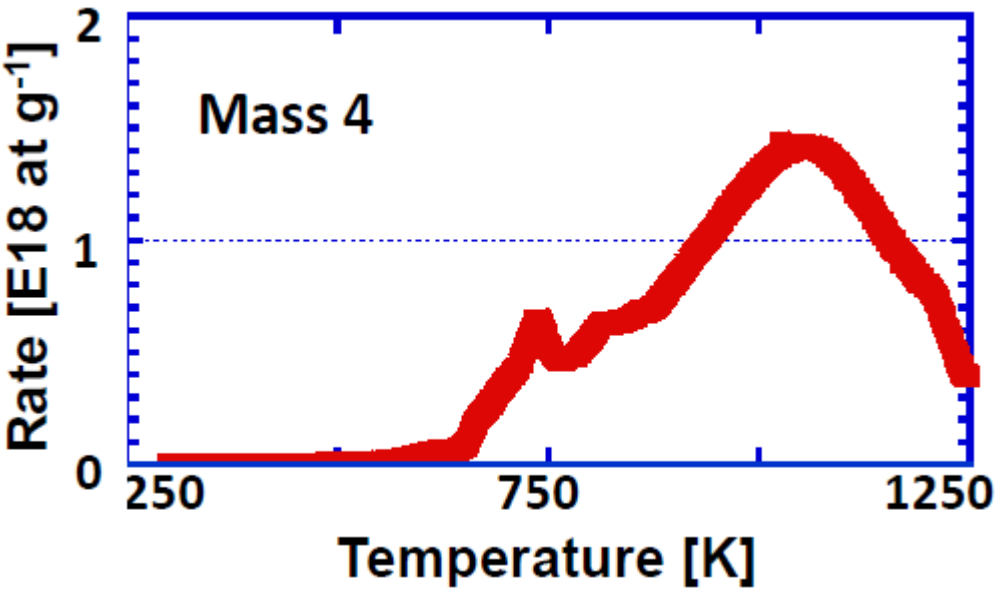

Figure 6

Surface topography and internal structure of tungsten dust sampled by sticky pads from the outer divertor tile recorded by SEM and STEM: (a) SEM image of surface features; (b) - (d) STEM images revealing details of the crystalline structure and porosity, (e) and (f) high resolution STEM revealing defects: dislocations and dislocation loops.

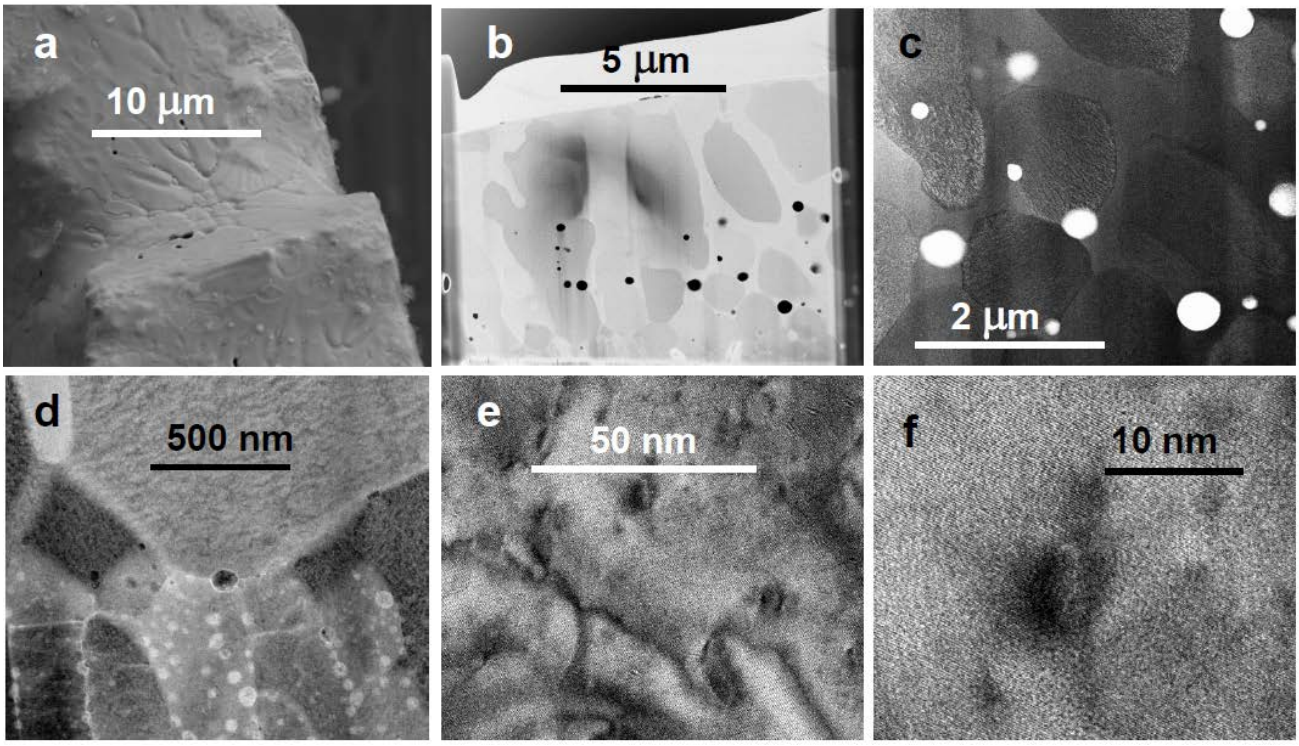

Figure 7

Thick beryllium deposits retrieved from the divertor carriers: (a) – (c) surface topography recorded by SEM and (d)-(g) internal structure recorded by STEM from the FIB-produced lamellae. Images (e) and (g) recorded in secondary electron mode, while (d) is high angle annular dark field image and (f) is a bright field image.

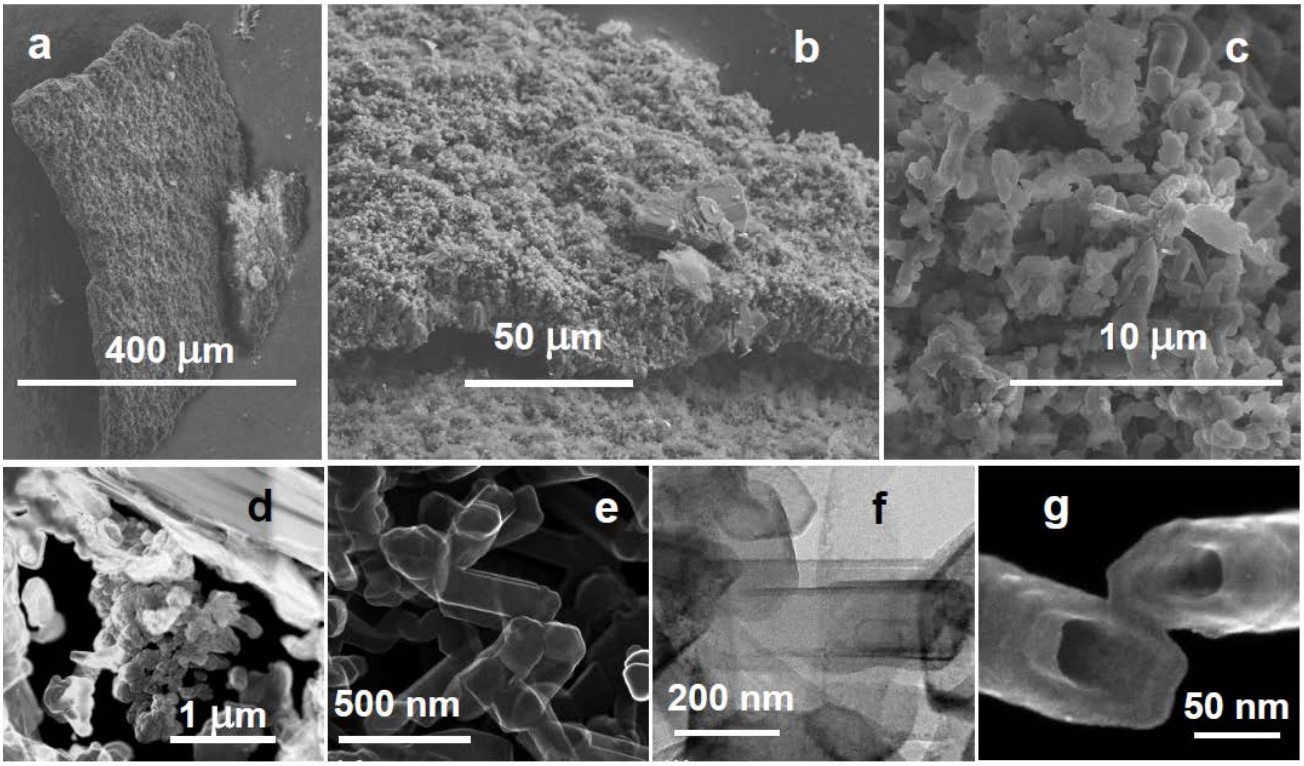

Figure 8.

Analysis of silicon plate of the dust monitor from the inner divertor: (a) HIERDA-based depth profiles of co-deposit constituents on the plate; (b) overview SEM image of the Si plate with deposited dust particles and the peeling-off layer the co-deposit.

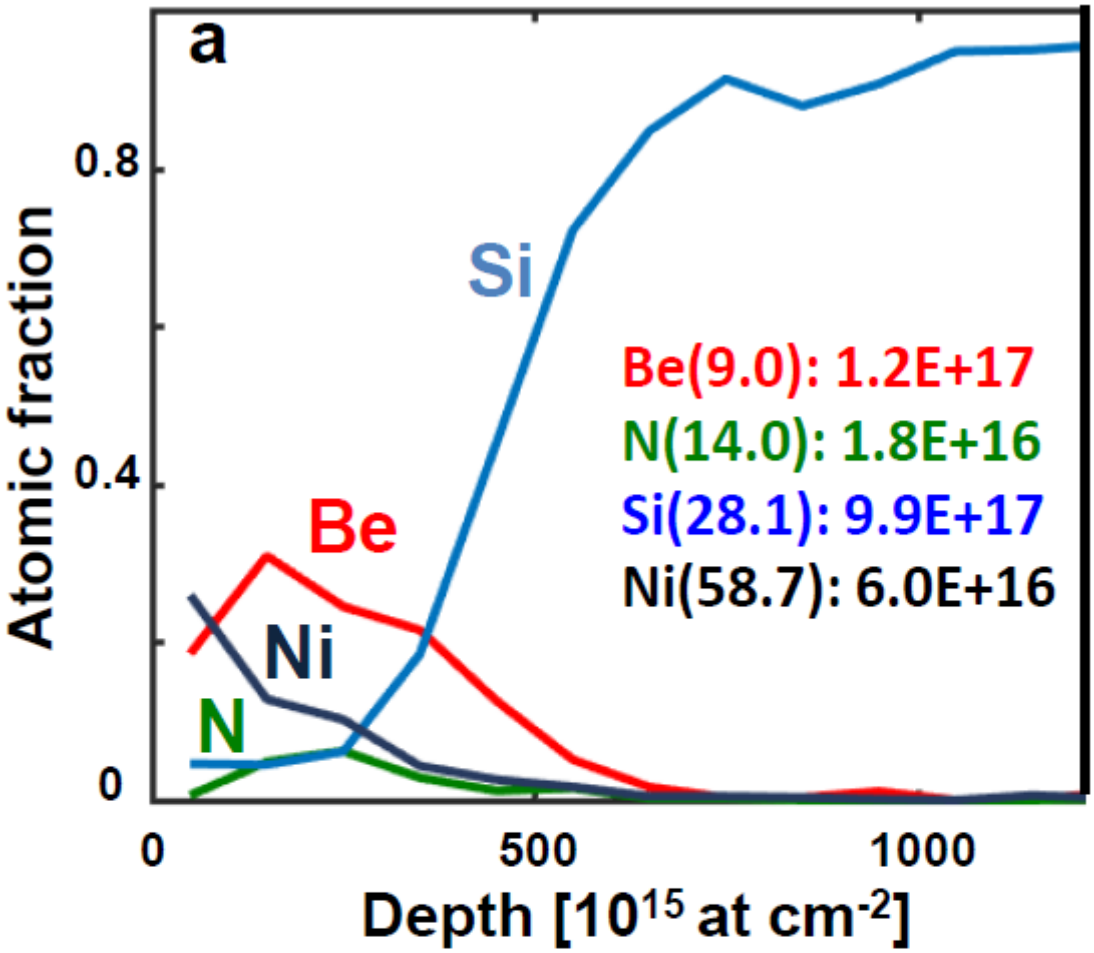

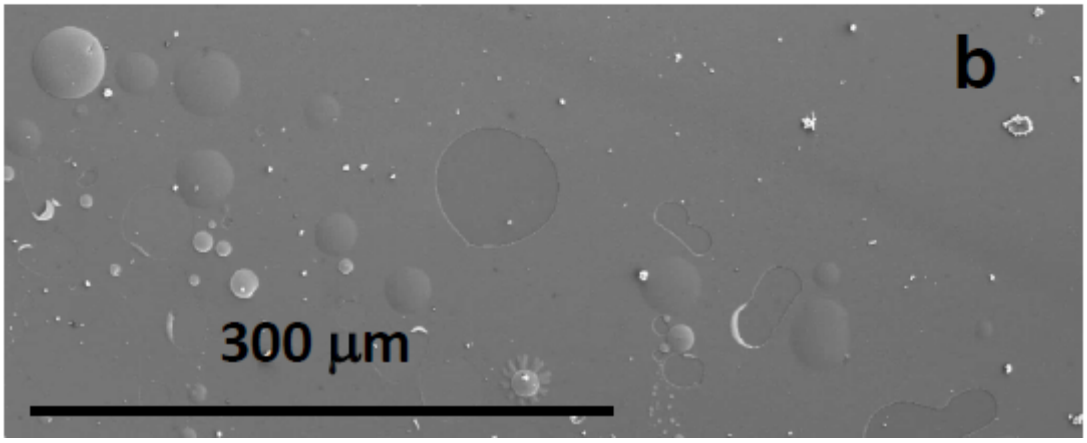

Figure 9.

SEM images of medium-Z and high-Z metal particles on the dust monitor: (a) and (b) nickel (Inconel) droplet and splash; (c) copper particle and (d) tungsten spherical particle formed the agglomeration of flakes from W-coated CFC tiles.

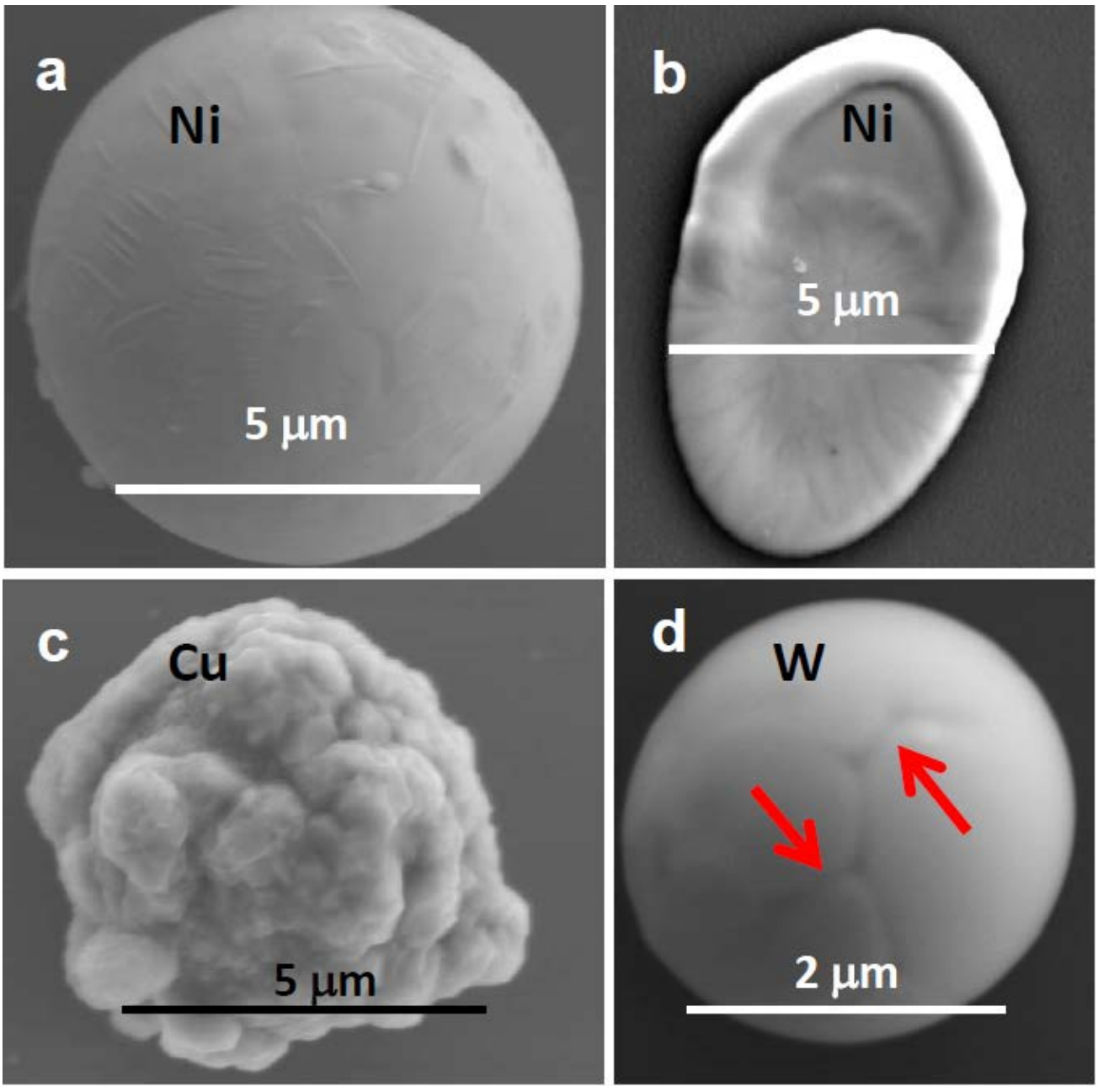

Figure 10.

SEM images of beryllium droplets and splashes: (a) splash on the dust monitor from the inner divertor (a); splash on the test mirror from the main chamber (b); droplets with surface features indicating the presence of cavities (c) and (d) small bubbles; (e) FIB-produced cross-section revealing the structure of thin-wall bubbles in a Be-rich deposit from the inner divertor; (f) bubble-like structure on the Be splash on the test mirror.